Characterization of Radioactive Aerosols Generated during Laser Cutting for Nuclear Power Plant Decommissioning

Joonsoo Ock [a], Wonseok Yang [b], Jae Sung Shin [c], Min-Ho Lee [d], Sungyeol Choi [a*]
[a] *Seoul National University, 1 Gwanak-ro, Gwanak-gu, Seoul 08826, Korea*
[b] *Korea Advanced Institute of Science and Technology, 291 Daehak-ro, Yuseong-gu, Daejeon 34141, Korea*
[c] *Korea Atomic Energy Research Institute 989-111 Daedeokdae-ro, Yuseong-gu, Daejeon 34057, Korea*
[d] *FNC Technology Co., Ltd., 13 Heungdeok 1-ro, Yongin-si, Gyeonggi-do, 16954, Korea*
[*]Corresponding author : choisys7@snu.ac.kr

***Keywords :** Radioactive aerosols, Laser cutting, Decommissioning and decontamination, Internal exposure

1. Introduction

Laser cutting technology is in the spotlight as an advanced solution for the Decontamination and Decommissioning (D&D) of nuclear power plants (NPPs). This is attributed to its capacity to offer greater precision, accuracy, and customization in contrast to conventional cutting methods such as plasma cutting, water jet cutting, and oxy-fuel cutting [1]. However, it is essential to emphasize that laser cutting operates through a thermal process, potentially resulting in the release of a large amount of radioactive aerosols. These aerosols play a critical role in increasing the potential for internal exposure among workers during the D&D process [2].

In order to effectively manage workers' internal exposure resulting from the inhalation of radioactive aerosols, specific parameters relevant to the particular working environment need to be defined, including aerosol-related values associated with physicochemical characteristics such as particle size and chemical composition [3]. This study aims to establish a system for collecting generated aerosol samples and for analysing physicochemical characteristics of aerosols during the process of laser cutting metal under various cutting conditions.

2. Experimental Setup and Methods

The aerosol sampling and measurement system (Fig. 1) comprises a 6 kW ytterbium fiber laser system, a sealed chamber with an automated cutting system, an aerosol sampling pipe applying isokinetic sampling, a diluter(eDiluter™, Dekati), a blower (manufactured), and a high-resolution low-pressure impactor device (HR-ELPI+, Dekati).

Stainless-steel metal, which is commonly used in nuclear facilities, was chosen and cut in a sealed chamber of ca. 1.65 m^3. To enhance experimental reproducibility, a HEPA filter was installed at the lower left corner of the chamber, aiming to create a controlled environment similar to a cleanroom.

To ensure the effective removal of residual aerosols within the chamber and rapid collection of generated aerosols to minimize aerosol loss, a sufficiently high flow velocity through the blower is required. Also, for accurately collecting a representative aerosol sample, isokinetic sampling is required [4]. Therefore, sampler heads of different sizes, along with an isokinetic sampler, were developed to achieve isokinetic sampling (Fig. 2). The diameter of the sampler head was determined based on the flow velocity at the sampling point. In this study, a sampling head with a diameter of 4 mm was installed as the flow velocity was selected to be 9.34 m/s.

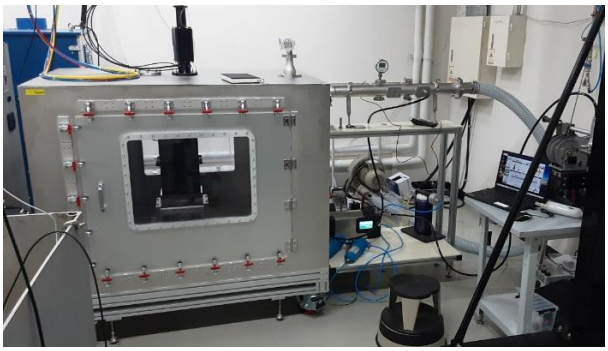

Fig. 1. The aerosol sampling and measurement system.

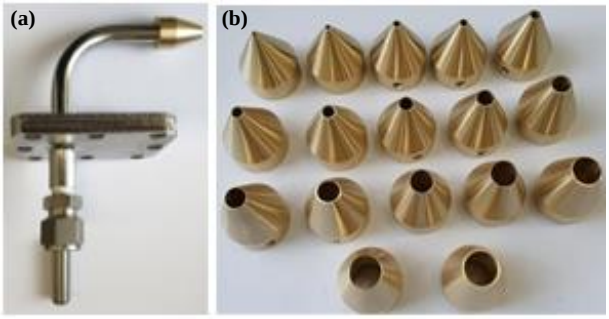

Fig. 2. (a) Isokinetic sampler, (b) Sampler heads

Based on prior research indicating negligible isotopic effects on aerosol size distribution [5], non-radioactive stainless-steel metal specimens were used in this study.

The experimental procedure involved a 10-minute blower operation to clear aerosols, followed by a 5-minute measurement of background aerosol levels. After setting and conducting cutting experiments, a 10-minute post-cutting measurement was conducted to ensure aerosol levels dropped back to the resting level. Aerosol samples were collected and size-classified using the HR-ELPI+ device, and then stored in conical tubes for

subsequent chemical composition analysis using ICP-MS.

3. Results and Discussions

3.1. Particle size distribution at different cutting speeds

Cutting experiments were conducted under cutting conditions (Table 1) based on the minimum required laser power for cutting at each thickness, in order to examine the influence of changing cutting speeds on particle size distribution. The speed ensuring a clean cut based on the metal thickness and laser power, obtained through several experiments, was chosen as the maximum speed applied in the experiments.

The variations in particle size distribution resulting from changes in cutting speeds for different conditions are depicted in Figure 3 and Figure 4. These conditions involve cutting metal thicknesses of 10 mm with a 1 kW laser power, 10 and 20 mm with 2 kW power, and 10, 20, and 30 mm with 3 kW power. Table 2 presents total aerosol number concentration, CMAD, and peak position values from the cutting experiments corresponding to Figure 3 and Figure 4.

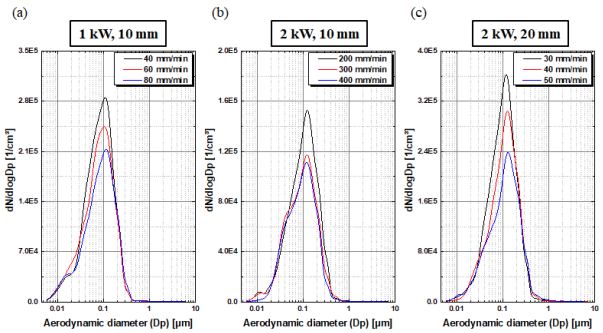

Fig. 3. Count aerodynamic distribution of aerosols generated by laser cutting process at different cutting conditions: (a) 1 kW, 10 mm thickness; (b) 2 kW, 10 mm thickness; (c) 2 kW, 20 mm thickness of stainless steel.

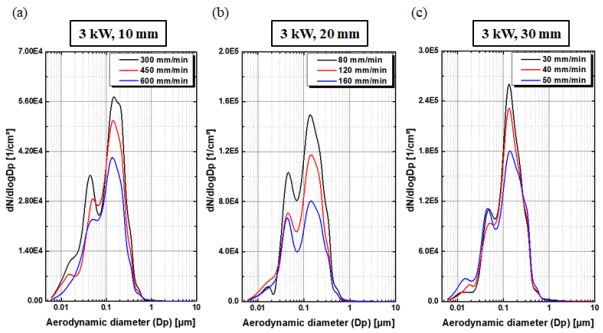

Fig. 4. Count aerodynamic distribution of aerosols generated by laser cutting process at different cutting conditions with 3 kW: (a) 10 mm thickness, (b) 20 mm thickness, (c) 30 mm thickness of stainless steel.

Table 1. Cutting speeds [mm/min] dependent on the minimum laser power according to the metal thickness.

Laser power (kW)	Metal thickness (mm)		
	10	**20**	**30**
1	40	-	-
	60		
	80		
2	200	30	-
	300	40	
	400	50	
3	300	80	30
	450	120	40
	600	160	50

Table 2. Total aerosol number concentration, CMAD, and peak position values for different cutting conditions obtained from HR-ELPI+ device.

Cutting conditions			Total N [d]	CMAD [e]	Peak position [f]
L [a]	T [b]	C [c]			
1	10	40	1.600E+08	0.083543	0.109117
		60	1.327E+08	0.082312	0.104367
		80	1.126E+08	0.087345	0.114084
2	10	200	6.842E+07	0.104367	0.122869
		300	5.611E+07	0.095477	0.122869
		400	5.160E+07	0.094071	0.121060
	20	30	2.053E+08	0.101315	0.119277
		40	1.640E+08	0.110748	0.126570
		50	1.311E+08	0.114084	0.130382
3	10	300	2.968E+07	0.110748	0.149099
		450	2.441E+07	0.112404	0.142522
		600	1.977E+07	0.105927	0.136317
	20	80	8.398E+07	0.115789	0.138354
		120	6.238E+07	0.114084	0.144652
		160	4.586E+07	0.107510	0.142522
	30	30	1.424E+08	0.124706	0.132331
		40	1.241E+08	0.124706	0.132331
		50	1.153E+08	0.119277	0.138354

[a] Laser power [kW].
[b] Thickness of the plate [mm].
[c] Cutting speed [mm/min].
[d] Total number concentration generation [1/cm^3].
[e] Count median aerodynamic diameter [μm].
[f] Particle size value at the highest peak [μm].

A notable point from Table 2 is that a clear trend of decreasing total aerosol number concentration with increasing cutting speed is identified, regardless of the metal thickness or laser power. As the cutting speed increases, the total aerosol number concentration shows a decrease, ranging from approximately 54.61% (cutting condition: 3 kW laser power, 10 mm metal thickness) to around 80.97% (cutting condition: 3 kW laser power, 30 mm metal thickness). This outcome is believed to be attributed to the increase in energy transferred to the metal plate as the cutting speed slows down.

On the other hand, for CMAD and the highest peak position values, it is concluded that the results based on different cutting speeds do not show a distinct trend.

3.2. Particle size distribution at practical maximum cutting speeds according to the laser power

We defined the practical maximum cutting speed as the maximum cutting speed that ensures a clean cut, established through multiple experiments. We analyze the variations in aerosol characteristics with respect to the practical maximum cutting speed for each laser power (1/2/3 kW) while keeping the metal thickness fixed at 10 mm. Table 3 presents the experimental results from the cutting experiments corresponding to Figure 6. We noticed a distinct decrease in total aerosol number concentration as laser output and practical maximum cutting speed increased. Conversely, CMAD values and the highest peak position indicated a shift toward larger particle sizes, suggesting a greater proportion of larger particles being produced.

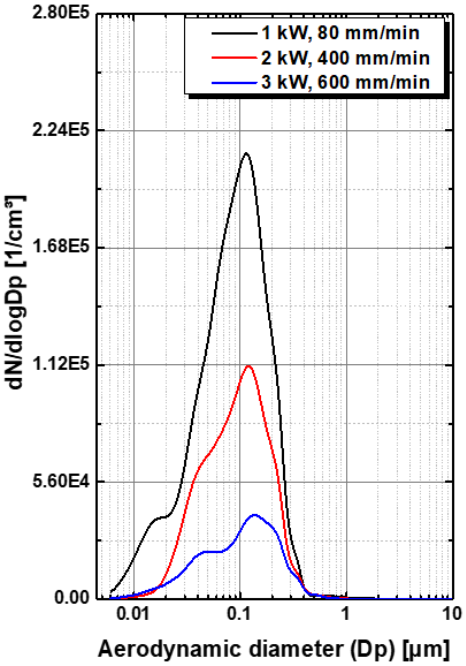

Fig. 6. Count aerodynamic distribution of aerosols generated by laser cutting process at different practical maximum cutting speeds.

Table 3. Total aerosol number concentration, CMAD, and peak position values for different practical cutting speeds according to the metal thickness obtained from HR-ELPI+ device.

Cutting conditions			Total N [d]	CMAD [e]	Peak position [f]
L [a]	T [b]	C [c]			
1	10	80	1.126E+08	0.087345	0.114084
2		400	5.160E+07	0.094071	0.121060
3		600	1.977E+07	0.105927	0.136317

[a] Laser power [kW].
[b] Thickness of the plate [mm].
[c] Cutting speed [mm/min].
[d] Total number concentration generation [1/cm³].
[e] Count median aerodynamic diameter [μm].
[f] Particle size value at the highest peak [μm].

4. Conclusion

In this study, we established an aerosol sampling and measurement system to collect aerosols generated during laser-cutting of stainless-steel metal specimens under various cutting conditions. A distinct trend of decreasing total aerosol number concentration with increasing cutting speed was observed, regardless of the metal thickness or laser power. The total aerosol number concentration decreased, ranging from approximately 54.61% to around 80.97%, depending on the specific cutting conditions. This phenomenon is believed to be attributed to the increase in energy transferred to the stainless-steel metal plate as the cutting speed slows down.

In the experimental results obtained using the practical maximum cutting speeds according to the laser power for metal plates of the same thickness (10mm), it was observed that as the cutting speed increased, the values of CMAD and the highest peak position showed a distinct trend towards larger sizes. Based on these results, it can be concluded that selecting the highest applicable laser power to achieve the fastest cutting speed is the most suitable approach.

Additional research will be conducted soon to calculate the committed effective dose coefficients for major nuclei using IMBA^{Lite} or the TAURUS internal dosimetry software, which reflects the latest ICRP recommendations. The aerosol characteristic data obtained from this study will be utilized as input values for TAURUS, along with the data to be obtained from chemical analysis (ICP-MS) and ICRP recommended parameters (including absorption type, respiration rate, working time, etc.) [6].

Acknowledgements

This work was supported by the National Research Foundation of Korea (NRF) Grant funded by the Korea government (MSIT) (Project Number: RS-2022-00155395)

REFERENCES

[1] He, Y. et al. (2022). Laser cutting technologies and corresponding pollution control strategy. *Processes*, 10(4), 732.
[2] Chae, N. et al. (2019). Aerodynamic diameter and radioactivity distributions of radioactive aerosols from activated metals cutting for nuclear power plant decommissioning. *Journal of hazardous materials*, 369, 727-745.
[3] Paquet, F. et al. (2015). ICRP Publication 130: Occupational intakes of radionuclides. *Annals of the ICRP*, 44(2), 5-188.
[4] Hinds, W. C. & Zhu, Y. (2022). *Aerosol technology: properties, behavior, and measurement*. John Wiley & Sons.
[5] Oki, Y. et al. (1994). Particle size and fuming rate of radioactive aerosols generated during the heat cutting of activated metals. *Applied radiation and isotopes*, 45(5), 553-562.
[6] Lee, H. Y. et al. (2022). Evaluation of workers' internal exposure because of inhalation of radioactive aerosols in a plasma melting facility by using IMBA and TAURUS codes. *Journal of Radioanalytical and Nuclear Chemistry*, 331(10), 4397-4404.